term probability of collision between NEAs and Earth. The risk of collision between NEAs and Earth is partially offset by the fact that the NEAs have higher inclinations than previously thought, because NEAs with higher inclinations are less likely to impact the Earth (*12*). The size and shape of the NEA population is important for understanding the collision hazard for Earth, and their availability for study by space missions and for utilization as space resources. The distribution of NEA inclinations could provide insight into where the NEAs formed and how they move through the solar system.

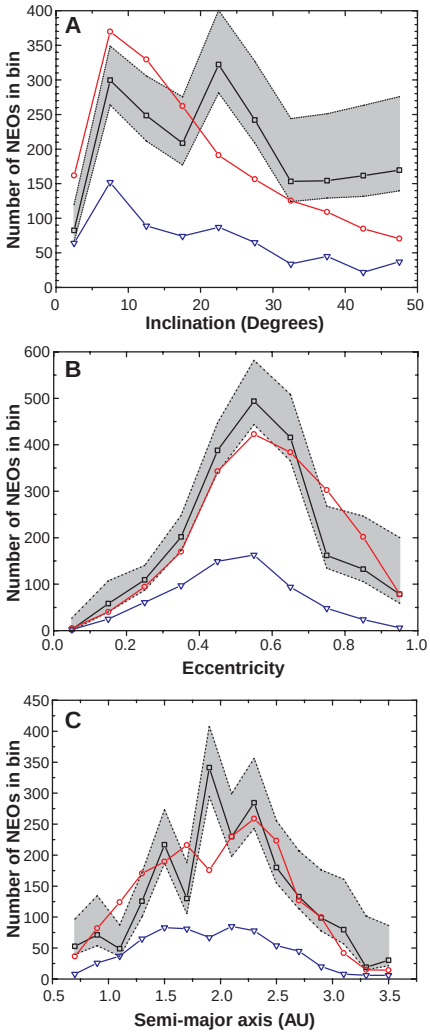

Fig. 3. Estimated distributions of the NEAs over the three orbital parameters: inclination (**A**), eccentricity (**B**), and semi-major axis (**C**). Each plot shows my estimate (black squares) of the population distribution with 1σ error bars (dotted lines and gray shading). Plotted for reference are the known NEAs (blue triangles) as of 9 October 2001 and the estimate recently published by Bottke *et al.* (*3*) (red circles). For comparison purposes, the curves from Bottke's model have been rescaled so that the total number of objects in the Bottke curves is the same as the total number of objects in the estimate given here. These curves include the estimates for the NEAs with $H < 18.5$ rather than $H < 18$ because the greatest number of detections used in this analysis fell within the $18.0 < H < 18.5$ bin. The spikes in the semi-major axis distribution are probably random fluctuation because they are consistent with the error envelope. The spikes in the inclination distribution are probably real because they appear in the known distribution.

References and Notes

1. The term near-Earth asteroids (NEAs) refers to asteroids with perihelia less than 1.3 AU, and aphelia greater 0.983 AU. This definition does not include objects with observable cometary comas or tails, although cataloged asteroids may include extinct comet nuclei.
2. W. F. Bottke, R. Jedike, A. Morbidelli, J. Petit, B. Gladman, *Science* **288**, 2190 (2000).
3. W. F. Bottke *et al.*, *Icarus*, in press.
4. D. Rabinowitz, E. Helin, K. Lawrence, S. Pravdo, *Nature* **403**, 165 (2000).
5. G. Stokes, J. Evans, H. Viggh, F. Shelly, E. Pearce, *Icarus* **148**, 21 (2000).
6. The LINEAR detection algorithm images each telescope field five times per night at half-hour intervals. Thus, 500,000 square degrees of coverage represents 2.5 million square degrees of imaging.
7. The integration times in this survey were selected to allow the system to cover 600 fields (about 1200 square degrees) while filling up the time available during the night. In winter, this allows for 11-s integration times, whereas in summer, as little as 3 s.
8. The a-e-i-H parameter space is broken into bins that are 0.1 AU wide in semi-major axis, 0.1 wide in eccentricity, 5° wide in inclination, and 0.5 magnitudes wide in absolute magnitude. For the plot in Fig. 3, the semi-major axis dimension was converted to bins 0.2 AU wide. The ranges of the parameters are 0.6 to 3.6 AU in semi-major axis, 0 to 1 in eccentricity, 0 to 50° in inclination, and 11 to 23 magnitudes in absolute magnitude. Bins with a-e values that do not meet the definition of NEA (*1*) are excluded.
9. The arguments of perihelion and the longitudes of the ascending node are assigned by a pseudo-random number generator producing a uniform distribution from 0° to 360°. The mean anomalies are evenly spaced from 0° to 360° at intervals of 0.5°.
10. I use the convention that absolute magnitude $H = 18$ corresponds to a diameter of 1 km. Absolute magnitude is the apparent brightness an object would have if placed at a theoretical position 1 AU from Earth and 1 AU from the Sun, with a Sun-asteroid-Earth phase angle of zero degrees. The correspondence of $H = 18$ with a diameter of 1 km is equivalent to using an albedo of 0.11, a widely assumed average value.
11. E. M. Shoemaker, R. F. Wolfe, C.S. Shoemaker, *Geol. Soc. Am. Spec. Paper 247* (1990), pp. 155–170.
12. E. J. Öpik, *Proc. R. Irish Acad.* **54A**,165 (1951).

13. Sponsored by the Department of the Air Force and NASA under Air Force Contract F19628-00-C-0002. Opinions, interpretations, conclusions, and recommendations are those of the author and are not necessarily endorsed by the United States Air Force. The author acknowledges financial support from the Lincoln Scholars Program at MIT Lincoln Laboratory. The author wishes to thank R. Binzel for guidance, F. Shelly and the telescope operators for collecting the data used in this analysis, and P. Hopman and R. Sayer for technical advice.

13 August 2001; accepted 12 October 2001

Dynamical Spreading of Asteroid Families by the Yarkovsky Effect

William F. Bottke Jr.,[1] David Vokrouhlický,[2] Miroslav Brož,[2] David Nesvorný,[1] Alessandro Morbidelli[3]

The orbital distributions of prominent asteroid families are thought to be direct by-products of catastrophic disruption events among diameter $D \gtrsim 100$ kilometer bodies. Ejection velocities derived from studying observed families, however, are surprisingly high compared with results from impact experiments and simulations. One way to resolve this apparent contradiction is by assuming that $D \lesssim 20$ kilometer family members, since their formation, have undergone semimajor axis drift by the thermal force called the Yarkovsky effect. Interactions between drifting family members and resonances can also produce unique eccentricity and/or inclination changes. Together, these outcomes help explain (i) why families are sharply bounded by nearby Kirkwood gaps, (ii) why some families have asymmetric shapes, and (iii) the curious presence of family members on short-lived orbits.

Catastrophic collisions among large asteroids in the main belt are believed to produce asteroid families [e.g., (*1*)]; clusters of asteroid fragments with similar proper semimajor axes a, eccentricities e, and inclinations i (*2*, *3*); and spectral signatures consistent with an origin from a common parent body (*4*, *5*). As such, prominent asteroid families (e.g., Koronis, Eos, Themis, Eunomia, and Vesta) are natural laboratories for understanding high-velocity impact physics, one of the principal geologic processes affecting small bodies in the solar system.

Although this formation scenario is straightforward, there are still many aspects of asteroid families that we do not yet under-

[1]Southwest Research Institute, 1050 Walnut Street, Suite 426, Boulder, CO 80302, USA. [2]Institute of Astronomy, Charles University, Prague, V Holešovičkách 2, 180 00 Prague 8, Czech Republic. [3]Observatoire de la Côte d'Azur, B.P. 4229, 06034 Nice Cedex 4, France.

*To whom correspondence should be addressed. E-mail: bottke@boulder.swri.edu

stand. We list a few below.

Up to now, the ejection velocities of observed asteroid family members have been derived under the assumption that the semimajor axes of these bodies have been relatively constant since the family was created (*6*, *7*). The diameter $D \lesssim 20$ km fragment velocities inferred from this technique are typically several 100 m s^{-1}. Curiously, these velocities are inconsistent with ejection velocities derived by other means. For example, numerical hydrocode experiments, which are capable of simulating hypervelocity collisions among large asteroids, indicate that mean ejection velocities of multikilometer fragments from family-forming impacts are ~100 m s^{-1} (*8*, *9*). Although limited data are available to validate these codes on large-scale asteroid collisions, they have successfully reproduced results ranging from laboratory impact experiments, where centimeter-sized projectiles are shot into targets, to underground nuclear explosions [e.g., (*8*)].

A second issue concerns the asymmetric and/or highly unusual (*a, e, i*) distributions of many asteroid families (*10*). As an example, we show the Koronis family in proper (*a*,*e*) and (*a*,*i*) (Fig. 1) (*11*). This family is nearly cut in two, with large proper *a* members more dispersed and actually offset in proper *e* than those with small proper *a*. In addition, both ends of the Koronis family are sharply bracketed by powerful mean motion resonances with Jupiter. Apparently, few observed family members have crossed either resonance, even though these resonances are relatively narrow when compared with the span of the family. This surprising coincidence cannot easily be explained in a simple scenario where the family's ejection velocity field has an upper cutoff.

A third issue involves the short-lived orbits of many family members. Several members of asteroid families are "on the brink" of entering a resonance [e.g., Koronis family members (*12*)], are already inside a powerful resonance [e.g., Eos family members (*5*)], or are part of the relatively short-lived near-Earth object population [V-type asteroids, which presumably were once part of the Vesta family before they escaped the main belt (*13*)]. Because the ages of families like Koronis, Eos, and Vesta are thought to be 1 billion years (Gy) or more (*14*), it is difficult to understand how these family fugitives reached orbits with such short dynamical lifetimes [~10 million years (My) or less (*15*, *16*)].

These inconsistencies, and recent advances in our understanding of asteroid dynamics, have motivated us to consider a modified scenario for producing families: Family members, rather than being static after ejection, instead undergo slow but steady migration by the Yarkovsky effect. The Yarkovsky effect is a thermal radiation force that causes objects to undergo semimajor axis drift as a function of their size, spin, orbit, and material properties (*17*). Analytical and numerical results show that this force can move an ensemble of $D = 5$ km asteroids inward and outward at mean drift rates of $|da/dt| \sim 2 \times 10^{-5}$ astronomical units (AU) My^{-1}, whereas larger asteroids drift more slowly (e.g., $D \sim 20$ km asteroids drift at $|da/dt| \sim 6 \times 10^{-6}$ AU My^{-1}) (*18*). These rates, which are relatively insensitive to the surface properties of the asteroids in the size regime considered, are in the right ballpark to explain the observed semimajor axis dispersions of most asteroid families, particularly those that are hundreds of My to Gy old (*14*). Moreover, because the magnitude of the Yarkovsky drift is size-dependent, the final semimajor axis distribution depends on the size of the objects, as observed in (*7*).

To check our hypothesis, we tracked the dynamical evolution of Koronis family member using the symplectic integration code SWIFT-RMVS3 (*19*), modified to accommodate Yarkovsky thermal forces (*17*). We concentrate on the Koronis family in this report primarily because it exhibits all of the singular features described above and because its low (*e*,*i*) values keep it far from most potential interlopers. Our family formation model results are described step by step below.

Step 1: catastrophic disruption. For our starting conditions, we assume that the catastrophic disruption of the Koronis parent body [$D = 119$ km (*20*)], arbitrarily placed at the orbit of (158) Koronis, ejected multikilometer-sized fragments at velocities ≲60 m s^{-1}. We purposely chose velocities lower than the inferred ejection velocities of observed Koronis family members [≲300 m s^{-1} (*7*)] or even those of hydrocode simulations [~100 m s^{-1} (*9*)] in order to gauge the importance of the Yarkovsky effect. For this reason, no attempt was made to match the (*e*,*i*) span of Koronis family values near, say, 2.87 AU, although more realistic initial conditions could readily do so. We tracked the evolution of 210 test asteroids with $2 < D <$ 40 km. The test asteroids were given random spin axis orientations, spin periods between 4 and 12 hours, and thermal and material properties consistent with regolith-covered asteroids such as Koronis family member (243) Ida (*21*, *22*).

Step 2: dynamical evolution in semimajor axis. Our fragments were numerically integrated for ~700 My, less than the assumed age of the Koronis family [2.5 to 3.0 Gy (*14*, *21*)] but long enough to determine evolutionary trends for slower drifting bodies (Fig. 2). After 100 My, most bodies have migrated in semimajor axis alone; few substantial changes in (*e*,*i*) are observed. Our largest fragments, being less susceptible to the Yarkovsky effect, do not move very far. We expect them to gain some limited mobility over the age of the family through processes such as collisions and/or close encounters with asteroids such as (1) Ceres, (2) Pallas, or (4) Vesta (*23*, *24*).

Step 3: interactions with weak resonances. Yarkovsky forces drive many family members through numerous resonances where resonant jumping/trapping events produce noticeable changes in proper eccentricity, particularly on the right side of Fig. 2. The most conspicuous effects are not caused by chaotic diffusion, because the widths of the few mean motion resonances existing in this region are tiny at small *e* values. Rather, the marked jumps are caused by interactions with secular resonances (e.g., $g + 2g_5 - 3g_6$ at 2.92 AU) that increase *e* but do not substantially change *i* (Fig. 1) (*25*). If the Yarkovsky effect did not exist, asteroids injected into the $g + 2g_5 - 3g_6$ resonance would undergo cyclic *e* oscillations until removed from resonance by a collision or a close encounter with a large asteroid. With Yarkovsky, on the other hand, bodies drifting into the left separatrix increase their *e* values until reaching the right separatrix, where they can jump out of the resonance. This outcome gives Koronis family members passing through the $g + 2g_5 - 3g_6$ resonance a permanent boost in *e*. Ultimately, the Yarkovsky effect splits the Koronis family into two distinct "clouds" in (*a*,*e*) space, with those on the right side predominately made up of small, fast-drifting objects

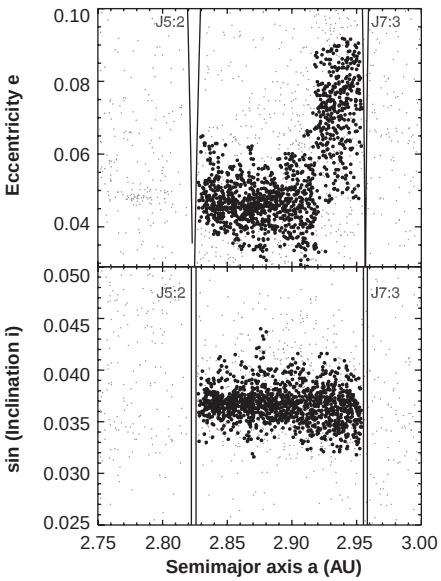

Fig. 1. Orbital distribution of 1322 Koronis family members (black dots) in proper semimajor axis *a* versus proper eccentricity *e* (**top**) and inclination *i* (**bottom**) (*11*). The gray dots are main belt asteroids having proper $e < 0.1$ and proper $\sin i < 0.05$. The family is bracketed by the 5:2 and 7:3 mean motion resonances with Jupiter. The left side of the 5:2 and the right side of the 7:3 show no substantial concentrations of asteroids in both (*a*,*e*) and (*a*,*i*) space.

(e.g., Fig. 1). Thus, the unusual (a,e) shape and size-orbit distribution of the Koronis family, together with the notable lack of dispersion in (a,i) space, provide strong evidence for asteroid mobility through the Yarkovsky effect.

Step 4: interaction with strong resonances. Figure 2 shows that Koronis family members drifting far enough within 700 My can become trapped in the powerful 5:2 or 7:3 mean motion resonances. By definition, these objects, with $D \sim 2$ km and obliquities near 0° or 180°, have the fastest drift rates in our simulation. Despite this, none are seen to jump across the 5:2 or 7:3 resonances. Thus, resonance capture events explain why no concentrations of family members are observed on the left/right sides of the 5:2/7:3 resonances, respectively (Fig. 1). Once captured, Koronis family members are pushed onto planet-crossing orbits, where they go on to strike the Sun or a planet, or are ejected from the inner solar system by a close encounter with Jupiter [e.g., (*16*)].

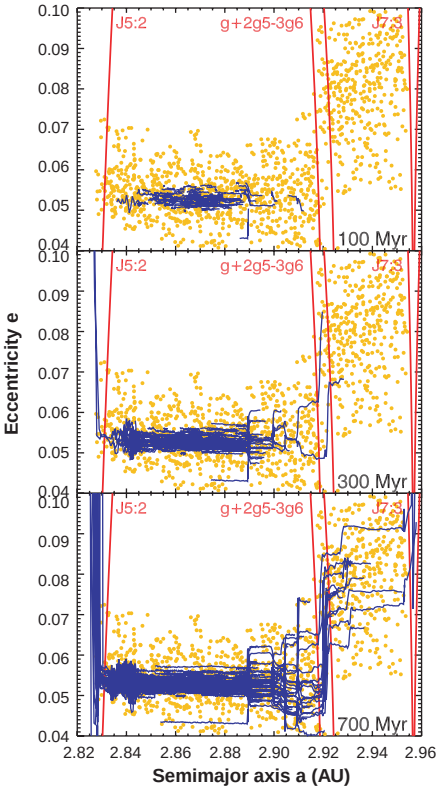

Fig. 2. Evolution of 210 simulated Koronis family members by the Yarkovsky effect. The test family members (blue lines) were started within ~60 m s^{-1} of (158) Koronis (proper elements a = 2.87 AU, e = 0.045, sin i = 0.038) and were integrated for ~700 My, short compared with the estimated age of the family (~2.5 Gy) but enough to determine evolution trends. The orbital tracks were averaged over a running 10-My window to compare them with the proper (a, e) of the Koronis family members (gold dots). Snapshots of the integration tracks, shown at 100, 300, and 700 My, indicate that these bodies interact with several resonances between 2.89 and 2.93 AU (*25*), with the secular $g + 2g_5 - 3g_6$ resonance at 2.92 AU being most prominent. These jumps allow the simulated family members to reach the (a,e) positions of many real family members. Fast-drifting bodies are seen to escape the main belt through the 5:2 and 7:3 mean motion resonances with Jupiter.

We believe our simulation reproduces the overall (a,e,i) distribution, the apparent size sorting of the Koronis family, and the paucity of family members on the left/right sides of the 5:2 and 7:3 resonances, respectively, while also showing that some Koronis family members could be escaping out of powerful resonances today [i.e., Koronis member (2953) Vysheslavia, a 15-km body, is located so close to the 5:2 resonance that it will be ejected from the main belt within 10 to 20 My (*26*)]. On the basis of these results, we conclude that the Yarkovsky effect, working in concert with resonances, can explain the mismatch between the observed spread of asteroid families such as Koronis and the size-velocity distributions derived from hydrocode simulations, all within a consistent model. The drawback with this paradigm, unfortunately, is that the current orbital distributions of $D \lesssim 20$ km bodies among most asteroid families cannot be directly used to infer the properties of the original breakup.

Our results imply that some asteroids observed in the Mars-crossing and/or near-Earth regions were family members produced billions of years ago by catastrophic disruption events. Thus, because Yarkovsky drift rates are size-dependant, large near-Earth asteroids such as (433) Eros could have taken billions of years to escape the main belt. This characteristic potentially explains why so few $D \gtrsim 20$ km near-Earth asteroids exist and why (433) Eros has such a heavily cratered surface. Initially, the Yarkovsky effect was introduced into planetary dynamics as a possible transportation mechanism for meteorites. Today, we are beginning to recognize that the Yarkovsky effect, together with resonances, may be the dominant means by which $D \lesssim 20$ km asteroids roam the main belt and reach the transportation resonances that can take them to the inner solar system (and Earth).

References and Notes

1. V. Zappalà, P. Bendjoya, A. Cellino, P. Farinella, C. Froeschlé, *Icarus* **116**, 291 (1995).
2. A. Milani, Z. Knežević, *Icarus* **107**, 219 (1994); Z. Knežević, A. Lemaitre, A. Milani, in *Asteroids III*, W. F. Bottke, A. Cellino, P. Paolicchi, R. Binzel, Eds. (Univ. of Arizona Press, Tucson, AZ, in press).
3. Proper elements are quasi-integrals of motion (i.e., they are nearly constant with time). They are obtained by eliminating the short- and long-term perturbations from osculating elements. An up-to-date list of nearly 70,000 asteroid proper elements can be found at the AstDyS information site (http://newton.dm.unipi.it).
4. R. P. Binzel, S. Xu, *Science* **260**, 186 (1993); A. Doressoundiram, M. A. Barucci, M. Fulchignoni, *Icarus* **131**, 15 (1998); D. Lazzaro *et al.*, *Icarus* **142**, 145 (1999).
5. V. Zappalà *et al.*, *Icarus* **145**, 4 (2000).
6. V. Zappalà, A. Cellino, A. Dell'Oro, F. Migliorini, P. Paolicchi, *Icarus* **124**, 156 (1996).
7. A. Cellino *et al.*, *Icarus* **141**, 79 (1999).
8. S. Love, T. J. Ahrens, *Icarus* **124**, 141 (1996); W. Benz, E. Asphaug, *Icarus* **142**, 5 (1999); E. Ryan, *Annu. Rev. Earth Planet. Sci.* **28**, 367 (2000).
9. P. Michel, W. Benz, P. Tanga, D. C. Richardson, *Science* **294**, 1696 (2001).
10. A. Morbidelli, V. Zappalà, M. Moons, A. Cellino, R. Gonczi, *Icarus* **118**, 132 (1995).
11. To distinguish the Koronis family from the background population, we applied a hierarchical clustering method to the modern proper element database found at the AstDyS information system (*3*). The criterion of family membership requires that all family members are connected by a "chain," where each member is located within a given velocity difference (cutoff) to its neighbor in proper (a,e,i). To be conservative, we chose 50 m s^{-1} as our cutoff velocity for family membership. A larger cutoff velocity of 100 m s^{-1} increases the number of outliers but does not substantially change the shape of the orbital distribution, mainly because the background population near the Koronis family is sparse. We find that our Koronis family has 1322 members with $1 < D <$ 46 km ($8.7 < H < 16.5$). Only a few objects near the lower D limit have been discovered. Our results are consistent with previous work (*1*).
12. A. Milani, P. Farinella, *Icarus* **115**, 209 (1995); Z. Knežević, A. Milani, P. Farinella, *Planet. Space Sci.* **45**, 1581 (1997).
13. F. Migliorini *et al.*, *Meteorit. Planet. Sci.* **32**, 903 (1997).
14. F. Marzari, D. Davis, V. Vanzani, *Icarus* **113**, 168 (1995); F. Marzari, P. Farinella, D. R. Davis, *Icarus* **142**, 63 (1999).
15. B. J. Gladman *et al.*, *Science* **277**, 197 (1997).
16. W. F. Bottke, R. Jedicke, A. Morbidelli, J. Petit, B. Gladman, *Science* **288**, 2190 (2000); W. F. Bottke *et al.*, *Icarus*, in press.
17. D. P. Rubincam, *J. Geophys. Res.* **100**, 1585 (1995); P. Farinella, D. Vokrouhlický, W. K. Hartmann, *Icarus* **132**, 378 (1998); W. F. Bottke, D. P. Rubincam, J. A. Burns, *Icarus* **154**, 301 (2000); D. Vokrouhlický, in *The Restless Universe: Applications of Gravitational N-Body Dynamics to Planetary, Stellar and Galactic Systems*, B. A. Steves, A. J. Maciejewski, Eds. (Institute of Physics, Bristol, UK, 2001), pp. 53–79.
18. P. Farinella, D. Vokrouhlický, *Science* **283**, 1507 (1999).
19. H. F. Levison, M. J. Duncan, *Icarus* **108**, 18 (1994); based on a symplectic algorithm by J. Wisdom, M. Holman, *Astron. J.* **102**, 1528 (1991).
20. P. Tanga *et al.*, *Icarus* **141**, 65 (1999).
21. R. Greenberg *et al.*, *Icarus* **120**, 106 (1996).
22. We assumed that our 210 fake Koronis family members had the following thermal and material properties: bulk densities of 2500 kg m^{-3}, surface densities of 1500 kg m^{-3}, thermal conductivity K = 0.001 W m^{-1} K^{-1}, specific heat C_p = 680 J kg^{-1}, emissivity ε = 0.9, and Bond albedo A = 0.10. Their spin periods were set to random values between P = 4 and 12 hours. One hundred twenty-five of our objects had $2 < D < 4$ km, 50 had between $4 < D < 8$ km, 25 had D = 16.5 km, and 10 had D = 37 km.
23. D. Nesvorný, A. Morbidelli, D. Vokrouhlický, W. F. Bottke, M. Brož, in preparation.
24. V. Carruba, J. Burns, W. F. Bottke, paper presented at Asteroids 2001, Palermo, Italy, 10 to 15 June 2001.
25. Secular resonances are defined with precession rates: those of the body of interest (the longitude of perihelion g and longitude of node s) and those of various planets (e.g., g_6 and s_6 are the fundamental frequencies of Saturn, the sixth planet). The $g + 3g_5 - 3g_6 - g_7$ resonance at ~ 2.91 AU, the $g + 2g_5 - 3g_6$ at ~ 2.92 AU, and the $g + g_5 - 3g_6 - g_7$ resonance at ~2.93 AU are responsible for many of the "jumps" in e observed in Fig. 2. The jumps seen near 2.9 AU are associated with the 12:5 mean motion resonance with Jupiter and several overlapping secular resonances. The reso-

nances responsible for the jumps at 2.89 AU have not yet been identified by our team, although they may be associated with various secular resonances and the weak 6:1 mean motion resonance with Saturn.

26. D. Vokrouhlický, M. Brož, P. Farinella, Z. Knežević, *Icarus* **150**, 78 (2001).

27. We thank V. Carruba, L. Dones, D. Durda, Z. Knežević, H. Levison, F. Marzari, P. Michel, A. Milani, F. Namouni, F. Roig, and D. Rubincam as well as our anonymous referees, for valuable contributions. Our work was strongly inspired by P. Farinella, a leading Italian planetary scientist who championed the importance of the Yarkovsky effect before his untimely death on 25 March 2000. We gratefully acknowledge the computational resources provided by the Cornell Theory Center. Research funds were provided by NASA grants NAG5-8950 and NAG5-9082 and European Space Agency contract 14018/2000/F/TB.

2 October 2001; accepted 24 October 2001

Collisions and Gravitational Reaccumulation: Forming Asteroid Families and Satellites

Patrick Michel,[1]* Willy Benz,[2] Paolo Tanga,[1,3] Derek C. Richardson[4]

Numerical simulations of the collisional disruption of large asteroids show that although the parent body is totally shattered, subsequent gravitational reaccumulation leads to the formation of an entire family of large and small objects with dynamical properties similar to those of the parent body. Simulations were performed in two different collisional regimes representative of asteroid families such as Eunomia and Koronis. Our results indicate that all large family members must be made of gravitationally reaccumulated fragments; that the post-collision member size distribution and the orbital dispersion are steeper and smaller, respectively, than for the evolved families observed today; and that satellites form frequently around family members.

Observed asteroid families in the main asteroid belt are of collisional origin (*1*). More than 20 asteroid families have been identified, each corresponding to groups of bodies concentrated in proper orbital element space (*2*) and sharing similar spectral properties (*3*). The theory of the collisional origin of asteroid families rests entirely on these similarities in dynamical and spectral properties and not on the understanding of the collisional physics itself. Despite several attempts (*4*), numerical simulations of fragmentation, although reproducing laboratory experiments on centimeter scale, have not been able to simultaneously explain the dynamical properties and the mass spectrum of asteroid families (*5*, *6*).

Here we explicitly simulate both the fragmentation of a parent body and the evolution of the debris cloud to late times, typically several days after fragmentation. We show that gravitational interactions between fragments result in reaccumulations (Fig. 1) and lead to the formation of a family of bound aggregates (*7*). This cluster, composed of well-dispersed "rubble piles"' (*8*) of all sizes, eventually evolves into one of today's asteroid families.

[1]Observatoire de la Côte d'Azur, B.P. 4229, 06304 Nice Cedex 4, France. [2]Physikalisches Institut, University of Bern, Sidlerstrasse 5, CH-3012 Bern, Switzerland. [3]Osservatorio Astronomico di Torino, Strada Osservatorio 20, 10025 Pino Torinese, Italy. [4]Department of Astronomy, University of Maryland, College Park, MD 20742–2421, USA.

*To whom correspondence should be addressed. E-mail: michel@obs-nice.fr

In our simulations, we model the family parent bodies as monolithic basalt objects, even though it is likely that they would have been shattered by the numerous small impacts taking place before a dispersing event. However, before being dispersed, our parent bodies are also shattered and, because gravity dominates over mechanical strength at these scales, this happens at correspondingly low energy costs (*9*). Consequently, although the collisional outcome may change in the details, we do not believe that the internal structure of the parent bodies can prevent reaccumulation from occurring.

The outcome of the collision is computed with a three-dimensional smooth particle hydrodynamics (SPH) code (*10*). This code solves in a Lagrangian framework the usual conservation equations (mass, momentum, and energy) in which the stress tensor has a nondiagonal part. We use the Tillotson equation of state for basalt (*11*, *12*), which is computationally expedient while sophisticated enough to allow its application over a wide range of physical conditions. Plasticity is introduced by modifying the stresses beyond the elastic limit with a von Mises yielding relation. For the lower tensile stresses associated with brittle failure, we use a fracture model based on the nucleation of incipient flaws, whose number density is given by a Weibull distribution (*13*, *14*).

Once the collision is over and fractures cease to propagate, the hydrodynamic simulations are stopped and intact fragments are identified. Typically, for the collisions considered here, the bodies are totally shattered into fragments of mass equal to our mass resolution. This corresponds to boulder sizes of ≈1 to 4 km. These fragments and their corresponding velocity distributions are fed into a gravitational *N*-body code, which computes the evolution of the system over the following days.

Because we are dealing with a large number of bodies (up to 2×10^5) that we want to follow over long periods of time, we use a parallel *N*-body hierarchical tree code (*15*) to compute the dynamics. The tree component of the code provides a convenient means of consolidating forces exerted by distant particles, reducing the computational cost. The parallel component divides the work evenly among available processors, adjusting the load at each time step according to the amount of work done in the previous force calculation. The code uses a straightforward second-order leapfrog scheme for the integration and computes gravity moments from tree cells to hexadecapole order. Collisions are identified at each step with a fast neighbor-search algorithm.

In order to keep the calculations tractable, we made some simplifications. We assume perfect sticking, which means that all colliding fragments are forced to stick regardless of their relative velocities (*16*). This assumption is justified because the initial impact results in an overall expanding cloud of fragments of relatively small individual masses, and colliding fragments have typical relative velocities that are smaller than their individual escape velocities. When two particles stick, they are merged into a single spherical particle with the same momentum.

Because the initial conditions that give rise to a particular family are unknown, we must proceed by trial and error until the outcome matches the characteristics of the largest family member. To speed up this phase of the process, we do not integrate the system to late times using the *N*-body code but rather apply an iterative procedure (*9*, *17*) to identify this largest member. Except in the cases where its mass represents less than 10% of the target's mass, this procedure has been successful at predicting its actual characteristics.

Our first aim was to create a family with a fairly large mass ratio of the largest remnant to the parent body M_{lr}/M_{pb}. A good example of such a family is Eunomia. The list of family members is thought to be complete for bodies with diameters larger than 11 km; there are 110 Eunomia members larger than this value (*18*–*20*). The estimated diameter of the parent body